

Jordan Journal of Physics

ARTICLE

Preparation of Nanocrystalline $\text{BaFe}_{12-2x}\text{Co}_x\text{Ti}_x\text{O}_{19}$ by Ball Milling Method and their Magnetic Properties

Ibrahim Bsoul

Department of Physics, Al al-Bayt University, Mafraq, Jordan.

Received on: 29/1/2009; Accepted on: 12/4/2009

Abstract: Nanocrystalline $\text{BaFe}_{12-2x}\text{Co}_x\text{Ti}_x\text{O}_{19}$ with $0 \leq x \leq 1$ were prepared by a simple method of ball milling. Magnetic and SEM measurements show that the coercive field and average grain size is decreasing with the increase of Co-Ti substitution. IRM and DCD curves were measured in order to investigate the role of doping with Co-Ti on the interactions between particles in $\text{BaFe}_{12-2x}\text{Co}_x\text{Ti}_x\text{O}_{19}$ samples using the δm technique. Interaction investigation shows that δm for all samples examined is negative, which means interparticle interactions that assists the reversal mechanisms (demagnetizing like effect).

Keywords: Ball milling, Barium ferrite, Coercive field, Magnetization.

Introduction

Barium hexaferrite with a chemical formula $\text{BaFe}_{12}\text{O}_{19}$ is one of the most important compositions for perpendicular magnetic recording. Barium hexaferrite is suitable for magnetic recording due to its large saturation magnetization, good chemical stability, and low switching field distribution. On the other hand, barium hexaferrite can be used for high density magnetic recording if its particle size and its large anisotropy field were decreased. Because large particle size and high anisotropy field causes a poor overwrite modulation [1]. In order to reduce the anisotropy field and to satisfy the desired applications, many studies were taken out to modify the magnetic properties of barium hexaferrite by the substitution of the Fe^{3+} ions with cations such as ($\text{Sn}^{4+}, \text{Ni}^{2+}, \text{Ni}^{3+}, \text{Co}^{2+}, \text{Co}^{3+}, \text{Ti}^{4+}, \dots$) [2-4] or cations combinations such as (Zn-Sn, Co-Sn [5, 6], Zn-Ti [7], Co-Ti [2], etc.).

Several techniques can be used to prepare barium ferrite powders such as the sol-gel method [8-10], the glass crystallization

method [11], hydrothermal technique [12], and coprecipitation method [13]. In the present work ball milling method was used to synthesize single-phase substituted nanocrystalline barium hexaferrite powder ($\text{BaFe}_{12-2x}\text{Co}_x\text{Ti}_x\text{O}_{19}$). The advantage of the above method is its operation simplicity and handy experimental apparatus. The preparation and investigation of barium ferrite doped with Co-Ti was reported in many works [14-17], but none of these works -to the knowledge of author- used the ball milling method. So in this work we have investigated the possibility of doping hexaferrites with ions such as Co-Ti by the ball milling route.

The structure of $\text{BaFe}_{12}\text{O}_{19}$ is of the form RSR^*S^* , Where R^* and S^* are obtained from the blocks R and S, by rotation of 180° around the hexagonal c axis. The ferric ions are distributed among five crystallographic sites. Three are octahedral sites ($12k, 4f_{IV}$, and $2a$); one is tetrahedral

site ($4f_{VI}$) and one trigonal bipyramid (2b)[18, 19].

Experimental procedures

The starting materials for synthesis of $BaFe_{12-2x}Co_xTi_xO_{19}$ ($x = 0, 0.2, 0.4, 0.6, 0.8$ and 1.0) were $BaCO_3$ (Aldrich-make), Fe_2O_3 (Aldrich-make), TiO_2 (Aldrich-make) and CoO (Aldrich-make). $BaFe_{12-2x}Co_xTi_xO_{19}$ compound was prepared in a planetary ball-mill (Fritsch Pulverisette 7) with balls and vial of hardened steel. The milling experiment was carried out at 250 rpm for 16 h and the ball to powder ratio was 8:1. The as-milled powders were annealed in air atmosphere at $1100^\circ C$ for 10 h. It should be noted that XRD analyses of more than 6 samples subjected to different annealing temperatures from $700^\circ C$ to $1200^\circ C$ revealed that the optimum annealing temperature for obtaining barium ferrite doped with Co-Ti was $1100^\circ C$. X-ray diffraction (XRD) analysis was carried out in Philips X'Pert PRO X-ray diffractometer (PW3040/60) with CuK_α radiation (45 kV, 40 mA). The obtained XRD data was compared with standard patterns of JCPDS-ICDD (International Center for Diffraction Data). The micrographs of the prepared samples were examined by the direct observation via

scanning electron microscopy (SEM) with EDX facilities (model FEI Quanta 600). The magnetic measurements were carried out using vibrating sample magnetometer (VSM) (MicroMag 3900, Princeton Measurements Corporation), with a maximum applied field of 795 kA/m. All magnetic measurements were performed at room temperature.

Results and discussion

Fig. 1 shows XRD patterns of Co and Ti doped barium ferrites ($BaFe_{12-2x}Co_xTi_xO_{19}$) with different doping concentration together with the standard pattern for $BaFe_{12}O_{19}$. The main diffraction peaks appearing in all XRD patterns can be indexed with the standard pattern for M-type hexagonal barium ferrite ($BaFe_{12}O_{19}$) with space group $P63/mmc$ (JCPDS file no: 043-0002), except a small peak at $2\theta = 33^\circ$ which belongs to Fe_2O_3 . In Table 1 we summarize the composition dependence of lattice parameters determined by X-ray diffraction and average crystallite size deduced from full width of half maximum using Scherrer's equation [20]. From these data we may propose that doping of barium ferrite with Co and Ti leads to an increase in lattice parameters and a decrease in average crystallite size.

TABLE 1. Lattice parameters and average crystallite size of $BaFe_{12-2x}Co_xTi_xO_{19}$, measured by XRD.

x	$a = b$ (Å)	c (Å)	Average crystallite size (D) nm
0	5.892	23.198	76
0.2	5.892	23.183	70
0.4	5.892	23.198	68
0.6	5.892	23.183	70
0.8	5.892	23.198	67
1.0	5.894	23.215	60

Fig. 2 shows the SEM photographs of Co and Ti doped barium ferrite powder with doping concentration of 0.0, 0.4 and 0.8. The grain size for the pure sample ($x = 0.0$) ranges from $0.2 \mu m$ to $1 \mu m$, while for $x = 0.8$ ranges from $0.2 \mu m$ to $0.6 \mu m$. So the average grain size tends to decrease with the increase of Co and Ti concentration i.e. Co and Ti doping results in inhibition of grain growth which

agrees with previous works [17, 19]. It is interesting that the particles stick to each other due to their magnetic attraction. So the particle sizes observed from SEM measurements seem to be larger than those measured by XRD. Also, the sample seems to form clusters rather than columns of stacked platelets, which indicates presence of negative interactions between particles.

Fig. 3 shows the measured hysteresis loops for some of the $\text{BaFe}_{12-2x}\text{Co}_x\text{Ti}_x\text{O}_{19}$ samples as a function of applied magnetic field. The magnetization curve for the non-substituted sample belongs to hard magnetic material with high coercive field strength of 334 kA/m. This value of the coercivity is in a good agreement with the previous reports such as sol-gel method [18], mechanical

alloying method [1] and ball milling method [21] of preparing barium ferrite. The effect of Co-Ti ions on the saturation magnetization and coercivity of $\text{BaFe}_{12-2x}\text{Co}_x\text{Ti}_x\text{O}_{19}$ are shown in Fig. 4. The saturation value of magnetization was obtained by extrapolating the magnetization versus $1/H$ to $1/H = 0$.

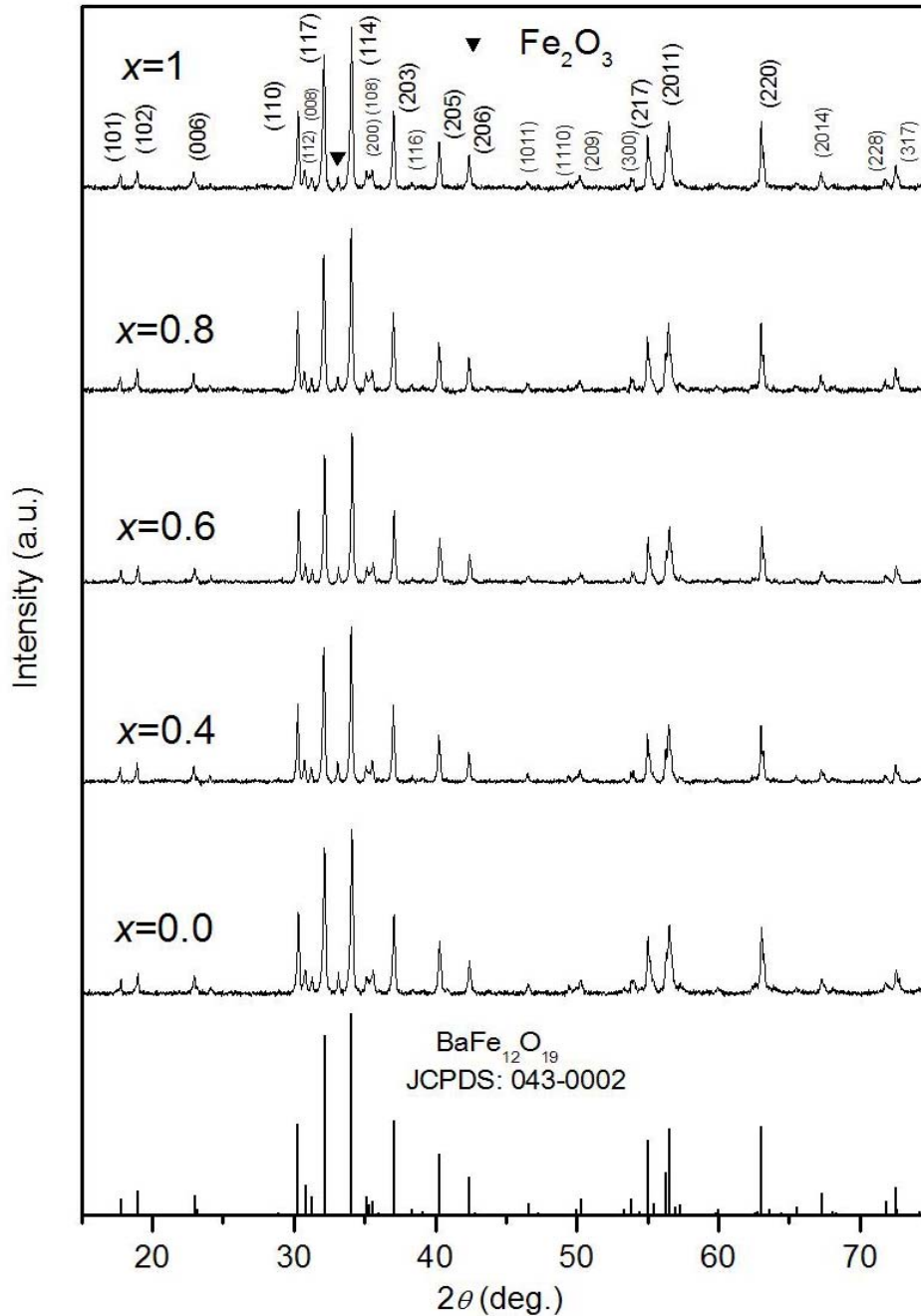


FIG. 1. Standard JCPDS pattern for M-type hexagonal barium ferrite (file no: 043-0002) and XRD patterns of $\text{BaFe}_{12-2x}\text{Co}_x\text{Ti}_x\text{O}_{19}$ with different doping concentration.

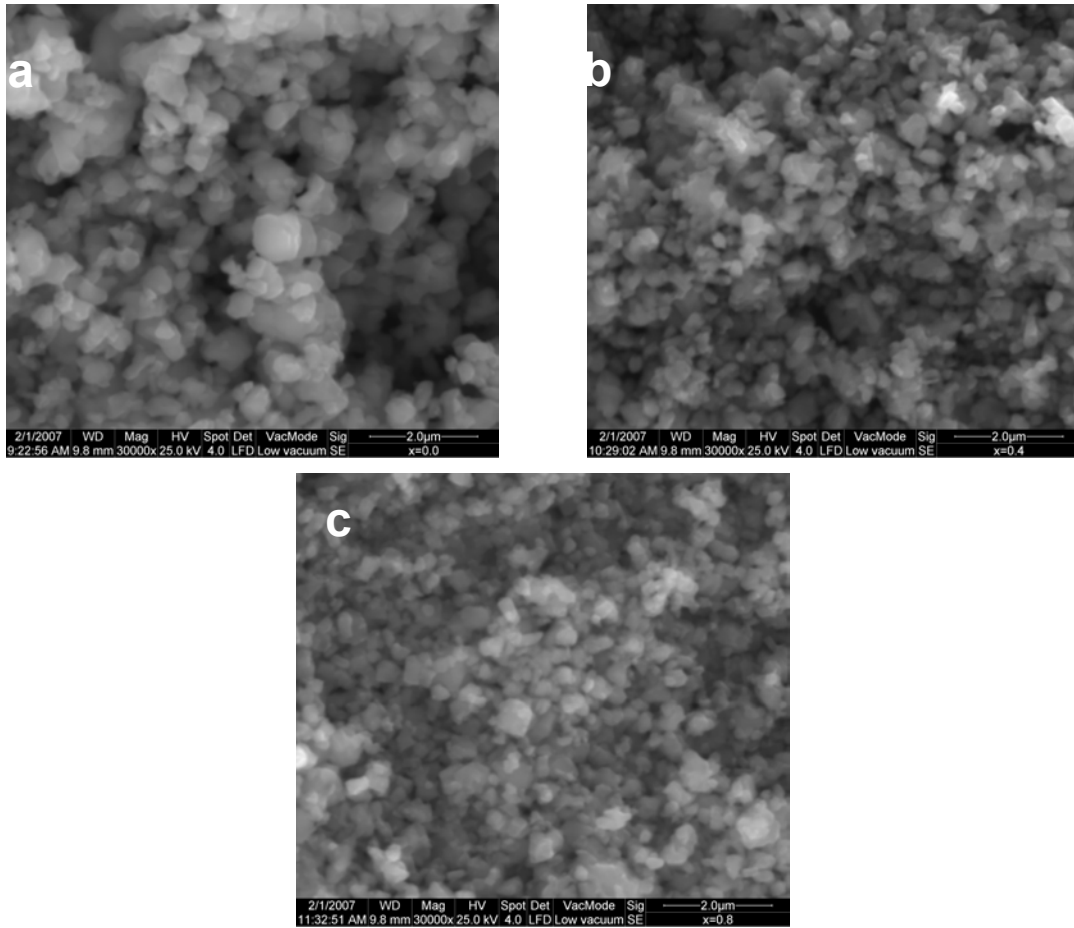


FIG. 2. SEM photograph of $\text{BaFe}_{12-2x}\text{Co}_x\text{Ti}_x\text{O}_{19}$, a) $x=0.0$, b) $x=0.4$ and c) $x=0.8$.

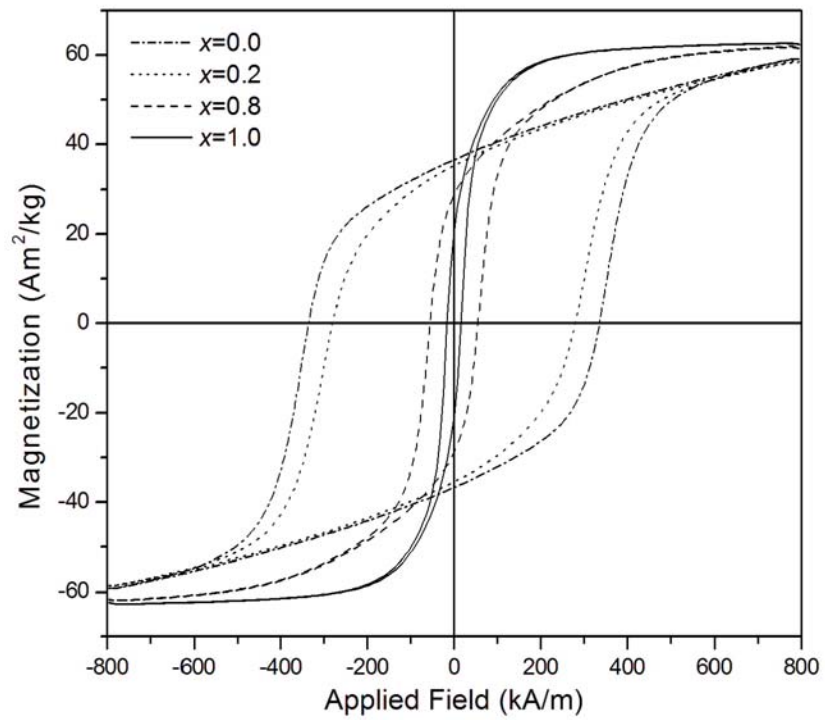


FIG. 3. Hysteresis loops for some of the $\text{BaFe}_{12-2x}\text{Co}_x\text{Ti}_x\text{O}_{19}$ samples as a function of applied magnetic field.

The saturation magnetization for the samples examined in this work ranges from 64 Am²/kg to 72 Am²/kg, which is higher than 50 Am²/kg reported by Radwan *et al.* [22], where they used chemical co-precipitation method for synthesis of barium ferrite powder. With increasing x the magnetization slightly decreases for all samples examined, which is suitable for applications such as perpendicular magnetic recording, microwave devices and material for permanent magnets where a high saturation magnetization is desired. While the coercivity drops dramatically from about 334 kA/m to 16

kA/m with the increasing of x from 0.0 to 1.0, which enables us to control the coercivity for various types of applications. As it was reported in literature [18, 23-25,] the iron ions at each of the five sites make a special contribution to the magnetic properties of BaFe₁₂O₁₉. A summary of these contributions is shown in Table 2. As one might see the major contribution to the coercivity comes from iron ions at 4f_{V1} and 2b. Therefore the dramatic drop of the coercivity (Fig. 4) can be referred to the replacement of Fe ions by Co and Ti ions at 4f_{V1} and 2b sites.

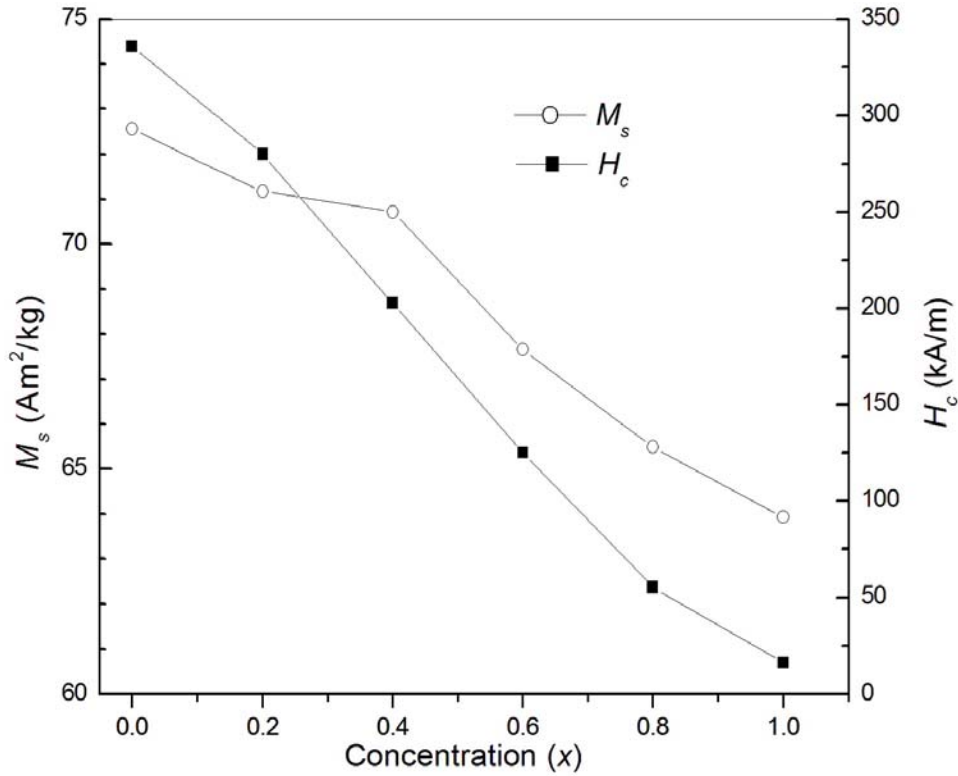


FIG. 4. Saturation magnetization and coercivity of BaFe_{12-2x}Co_xTi_xO₁₉ as a function of the concentration (x).

TABLE 2. Magnetic properties of crystallographic sites in barium ferrite (BaFe₁₂O₁₉).

Sites	Coordination	Spin direction	Contribution
4f _{V1}	octahedral	down	coercivity
2b	bipyramid	up	coercivity
4f _{IV}	tetrahedral	down	magnetization
12k	octahedral	up	temperature dependence of magnetization
2a	octahedral	up	

In order to investigate the role of doping with Co-Ti on the interaction effects we use δM relationship given by Kelly [26]:

$$\delta m(H) = m_d(H) - [1 - 2m_r(H)] \quad (1)$$

where $m_r(H) = M_r(H)/M_r(\infty)$ is the reduced isothermal remnant magnetization (IRM) and $m_d(H) = M_d(H)/M_r(\infty)$ is the reduced dc demagnetization (DCD). The IRM curve was obtained by the following

procedure: first the sample was demagnetized, second applying positive field, third measuring the remanence magnetization after removing the applied field. The procedure was repeated with increasing the positive field to reach positive saturation remanence. The DCD curve was obtained by, first, the sample was saturated with a positive field of 795 kA/m, second a negative field was applied to the sample, third, the remanence magnetization was recorded after removing the negative field and at last this procedure was repeated with increasing the negative field until negative saturation remanence was reached. The IRM and DCD curves for all samples examined in this work are shown in Fig. 5. By substituting these curves in eq. 1, we can obtain δm curves, which give the strength and the sign of the interaction in the prepared samples. For non interacting systems δm plots will show a horizontal line, any deviation from linearity in δm is a sign for the existence of

interparticle interactions. Positive δm values indicate the existence of interparticle interactions that contribute constructively to the magnetization (magnetizing like effect), i.e. particles tend to stack in column, while negative δm values suggest that the existing interactions are demagnetizing (demagnetizing like effect), i.e. particles tend to form clusters. Fig. 6 shows the δm curves as a function of the applied field for samples with different doping concentration of Co-Ti. As one can observe δm for all samples are negative for all fields, which agree with SEM observation of cluster formation. Also δm exhibit a maximum negative values at a field around coercivity. As one might observe the maximum negative value of δm exhibits minimum at $x = 0.4$ and 0.6 . This behavior needs a further investigation to clarify the influence of doping on the strength of interparticle interactions.

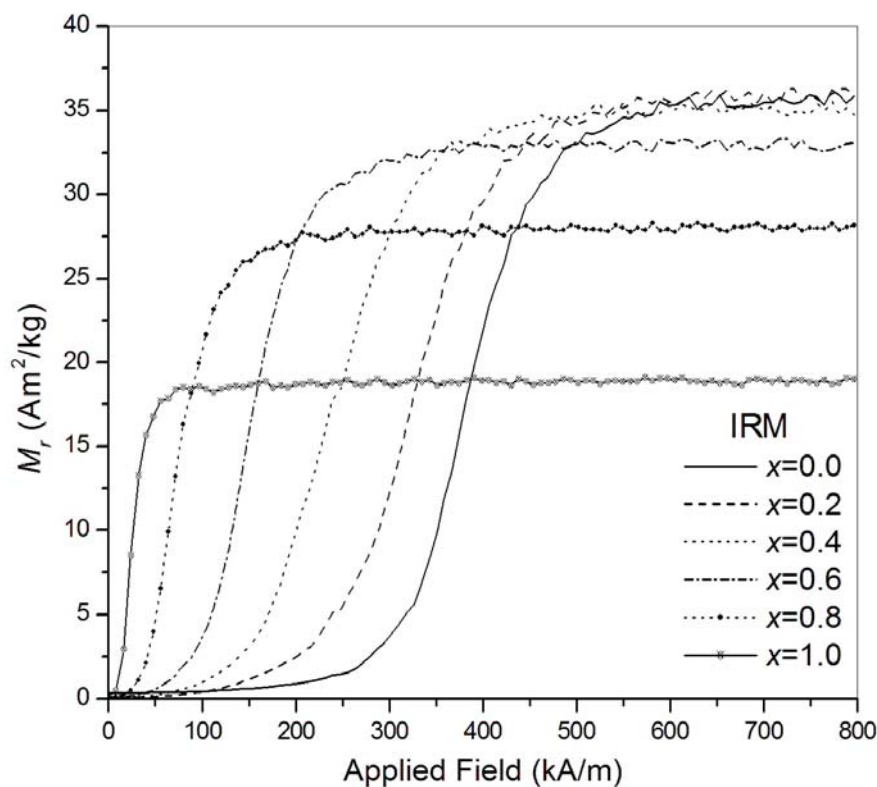


FIG. 5A. IRM curves of $\text{BaFe}_{12-2x}\text{Co}_x\text{Ti}_x\text{O}_{19}$.

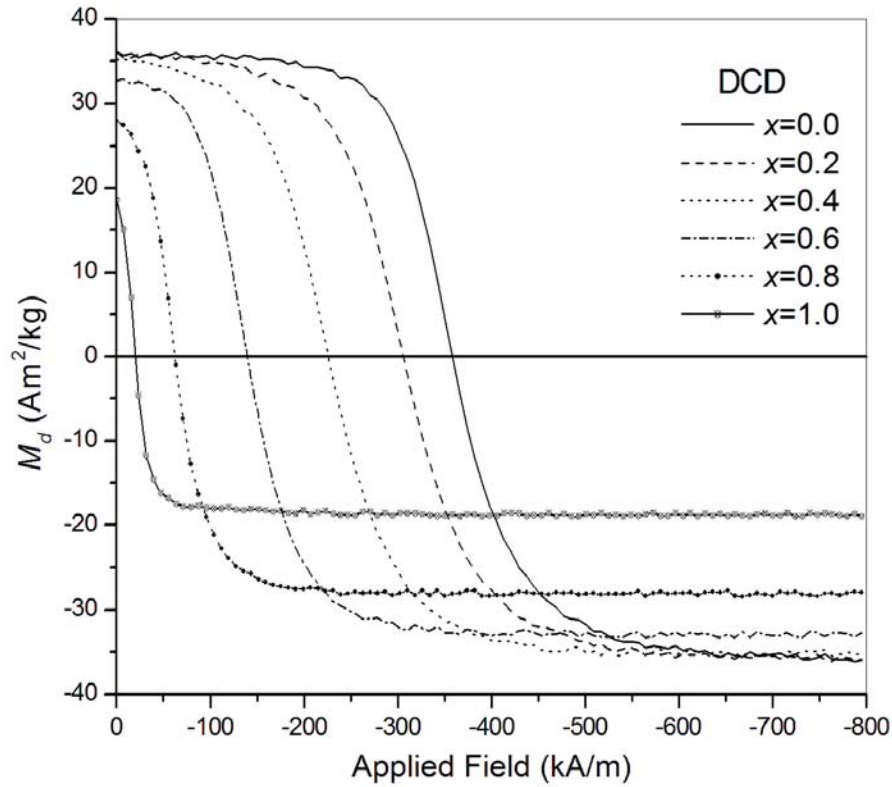


FIG. 5B. DCD curves of $\text{BaFe}_{12-2x}\text{Co}_x\text{Ti}_x\text{O}_{19}$.

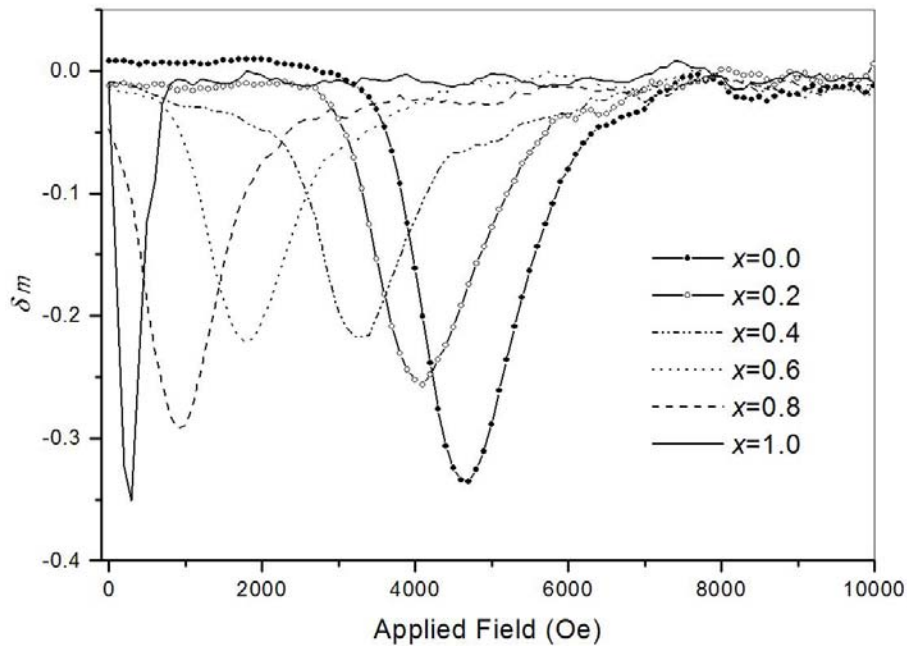


FIG. 6. δm curves of $\text{BaFe}_{12-2x}\text{Co}_x\text{Ti}_x\text{O}_{19}$ for some of the concentration examined

Conclusion

Nanocrystalline barium ferrite doped with Co-Ti ($\text{BaFe}_{12-2x}\text{Co}_x\text{Ti}_x\text{O}_{19}$) have been prepared using a very simple method of ball milling. It was found that doping of barium ferrite with Co-Ti leads to a significant decrease in the coercive field and inhibition of grain growth. Interaction investigation

show that δm for all samples examined is negative, which means interparticle interactions that assists the reversal mechanisms (demagnetizing like effect).

Acknowledgment

This work was supported by Deanship of Academic Research at Al al-Bayt University (Grant No. 213/2004/2005).

References

- [1] Sharma, P., Rocha, R.A., de Medeiros, S.N. and Paesano Jr, A., *Journal of Alloys and Compounds*, 443(1-2) (2007) 42.
- [2] Gruskova, A., Slama, J., Dosoudil, R., Kevicka, D., Jancarik, V. and Toth, I., *J. Magn. Magn. Mater.* 242–245 (2002) 423.
- [3] An, S.Y., Shim, I.B. and Kim, C.S., *J. Appl. Phys.* 91 (2002) 8465.
- [4] Marino-Castellanos, P.A., Somarriba-Jarque, J.C. and Anglada-Rivera, J., *Physica B: Cond. Mat.* 362 (2005) 95.
- [5] Yang, Z., Zeng, H.X., Han, D.H., Liu, J.Z. and Geng, S.L., *J. Magn. Magn. Mater.* 115 (1992) 77.
- [6] Han, D.H., Yang, Z., Zheng, H.X., Zhou, X.Z. and Morrish, A.H., *J. Magn. Magn. Mater.* 137 (1994) 191.
- [7] Wartewig, P., Krause, M.K., Esquinazi, P., Rosler, S., Sonntag, R., *J. Magn. Magn. Mater.* 192 (1999) 83.
- [8] Surig, C., Hempel, K.A. and Sauer, Ch., *J. Magn. Magn. Mater.* 157–158 (1996) 268.
- [9] Zhong, W., Ding, W., Zhang, N., Hong, J., Yan, Q. and Du, Y., *J. Magn. Magn. Mater.* 168 (1997) 196.
- [10] Garcia, R.M., Ruiz, E.R., Rams, E.E. and Sanchez, R.M., *J. Magn. Magn. Mater.* 223 (2001) 133.
- [11] El-Hilo, M., Pfeiffer, H., O'Grady, K., Schuppel, W., Sinn, E., Gornert, P., Rosler, M., Dickson, D.P.E. and Chantrell, R.W., *J. Magn. Magn. Mater.* 129 (1994) 339.
- [12] Liu, X., Wang, J., Gan, L.M. and Ng, S.C., *J. Magn. Magn. Mater.* 195 (1999) 452.
- [13] Zhao, W.Y., Zhang, Q.J., Li, L.C. and Guan, J.G., *J. Magn. Magn. Mater.* 295 (2005) 21.
- [14] Koga, N. and Tsutaoka, T., *J. Magn. Magn. Mater.* 313 (1) (2007) 168.
- [15] The, G.B., Saravanan, N. and Jefferson, D.A., *Materials Chemistry and Physics*, 105(2-3) (2007) 253.
- [16] Kakizaki, K., Hiratsuka, N. and Namikawa, T., *J. Magn. Magn. Mater.* 176 (1997) 36.
- [17] Yang, Z., Zeng, H.X., Han, D.H., Liu, J.Z., Geng, S.L., *J. Magn. Magn. Mater.* 115 (1992) 77.
- [18] An, S.Y., Shim, I.B. and Kima, C.S., *J. Appl. Phys.* 91(10) (2002).
- [19] Zhou, X.Z., Morrish, A.H., Li, Z.W. and Hong, Y.K., *IEEE Transactions on Magnetism*, 27(6) (1991).
- [20] Warren, B.E. "X-Ray Diffraction", (Addison-Wesley, Reading Massachusetts, 1969) p.253.
- [21] Babu, V., Padaikathan, P., *J. Magn. Magn. Mater.* 241 (2002) 85.
- [22] Radwan, M., Rashad, M.M. and Hessien, M.M., *Journal of Materials Processing Technology*, 181 (2007) 106.
- [23] Kim C.S., An, S.Y., Son, J.H., Lee, J.G. and Oak, H.N., *IEEE Transactions on Magnetism*, 35(5) (1999) 3160.
- [24] Zhou, X.Z., Morrish, A.H., Li, Z.W. and Hong, Y.K., *IEEE Transactions on Magnetism*, 27(6) (1991) 4654.
- [25] Turilli, G., Licci, F., Rinaldi, S. and Deriu, A., *J. Magn. Magn. Mater.* 59(1-2) (1986) 127.
- [26] Kelly, P.E., O'Grady, K., Mayo, P.I. and Chantrell, R.W., *IEEE Transactions on Magnetism*, 25(5) (1989) 3881.